Journal of Medicinal Chemistry

Article

pubs.acs.org/jmc

Synthesis and Anti-Renal Fibrosis Activity of Conformationally Locked Truncated 2-Hexynyl-N^6-Substituted-(*N*)-Methanocarba-nucleosides as A_3 Adenosine Receptor Antagonists and Partial Agonists

Akshata Nayak,[†,‡] Girish Chandra,[‡] Inah Hwang,[‡] Kyunglim Kim,[‡] Xiyan Hou,[‡] Hea Ok Kim,[‡] Pramod K. Sahu,[‡] Kuldeep K. Roy,[‡] Jakyung Yoo,[‡] Yoonji Lee,[‡] Minghua Cui,[‡] Sun Choi,[‡] Steven M. Moss,[§] Khai Phan,[§] Zhan-Guo Gao,[§] Hunjoo Ha,[‡] Kenneth A. Jacobson,[§] and Lak Shin Jeong*[,†,‡]

[†]Research Institute of Pharmaceutical Sciences, College of Pharmacy, Seoul National University, Seoul 151-742, Korea

[‡]College of Pharmacy, Graduate School of Pharmaceutical Sciences and Global Top 5 Research Program, Ewha Womans University, Seoul 120-750, Korea

[§]Molecular Recognition Section, Laboratory of Bioorganic Chemistry, National Institute of Diabetes, and Digestive and Kidney Disease, National Institutes of Health, Bethesda, Maryland 20892, United States

Supporting Information

ABSTRACT: Truncated N^6-substituted-(*N*)-methanocarba-adenosine derivatives with 2-hexynyl substitution were synthesized to examine parallels with corresponding 4′-thioadenosines. Hydrophobic N^6 and/or C2 substituents were tolerated in A_3AR binding, but only an unsubstituted 6-amino group with a C2-hexynyl group promoted high hA_{2A}AR affinity. A small hydrophobic alkyl (**4b** and **4c**) or N^6-cycloalkyl group (**4d**) showed excellent binding affinity at the hA_3AR and was better than an unsubstituted free amino group (**4a**). A_3AR affinities of 3-halobenzylamine derivatives **4f**−**4i** did not differ significantly, with K_i values of 7.8−16.0 nM. N^6-Methyl derivative **4b** (K_i = 4.9 nM) was a highly selective, low efficacy partial A_3AR agonist. All compounds were screened for renoprotective effects in human TGF-β1-stimulated mProx tubular cells, a kidney fibrosis model. Most compounds strongly inhibited TGF-β1-induced collagen I upregulation, and their A_3AR binding affinities were proportional to antifibrotic effects; **4b** was most potent (IC_{50} = 0.83 μM), indicating its potential as a good therapeutic candidate for treating renal fibrosis.

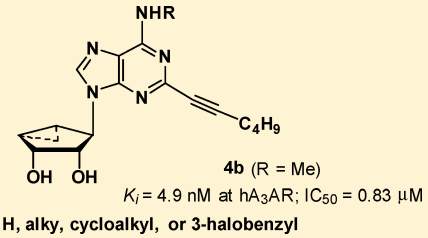

INTRODUCTION

Extracellular adenosine acts as a signaling molecule with a generally cytoprotective function in the body. Adenosine mediates cell signaling through binding to four known subtypes (A_1, A_{2A}, A_{2B}, and A_3) of adenosine receptors (ARs).[1−4] A_1, A_{2A}, and A_3ARs are activated by low levels of adenosine (EC_{50} = 0.01−1.0 μM) similar to physiological levels of adenosine, whereas A_{2B}AR is activated by high levels of adenosine (EC_{50} = 24 μM).[5] A_1 and A_3ARs are G_i-coupled G protein-coupled receptors (GPCRs), and A_{2A} and A_{2B}ARs are G_s-coupled GPCRs. Binding of adenosine to the ARs modulates second messengers such as adenosine 3′,5′-cyclic phosphate (cAMP), inositol triphosphate (IP_3), and diacylglycerol (DAG).[1−5] For example, the G_i-coupled A_3AR inhibits adenylate cyclase (AC), resulting in cAMP down-regulation, while it stimulates phospholipase C (PLC), which increases the levels of IP_3 and DAG. Therefore, ARs have been attractive targets for the development of new therapeutic agents related to cell signaling.

Chronic kidney disease (CKD) is characterized by kidney fibrosis and is becoming a major health problem worldwide,[6] and the use of renin−angiotensin−aldosterone system (RAAS) inhibitors[7,8] is one of a few therapeutic options for the treatment of CKD. However, the efficacy of RAAS inhibitors is limited;[9] it is, therefore, highly desirable to develop new therapeutic agents to improve the prognosis of CKD patients. Extracellular adenosine in the kidney dramatically increases in response to renal hypoxia and ischemia, and increased adenosine has been reported to be associated with CKD.[10] ARs were upregulated in unilateral ureteral obstructed rat kidneys, which is a well-characterized model of CKD,[11] and A_3AR knockout mice were protected against ischemia- and myoglobinuria-induced kidney failure.[10] Therefore, A_3AR antagonists may become effective renoprotective agents for the treatment of CKD.

Adenosine as a natural ligand has served as a good lead for the development of new AR ligands.[5] Extensive modifications on the N^6 and/or 4′-CH_2OH of adenosine have been explored, giving several potent and selective A_3AR agonists[12,13] such as N^6-(3-iodobenzyl)-5′-*N*-methylcarbamoyladenosine (IB-

Received: October 2, 2013
Published: January 24, 2014

   dx.doi.org/10.1021/jm4015313 | *J. Med. Chem.* 2014, 57, 1344−1354

MECA),[14] 2-chloro-N^6-(3-iodobenzyl)-5′-*N*-methylcarbamoyl-adenosine (Cl-IB-MECA),[15] N^6-(3-iodobenzyl)-5′-*N*-methyl-carbamoyl-4′-thioadenosine (thio-IB-MECA),[16] 2-chloro-N^6-(3-iodobenzyl)-5′-*N*-methylcarbamoyl-4′-thioadenosine (thio-Cl-IB-MECA),[17] and 3′-amino-N^6-{5-chloro-2-(3-methyl-isoxazol-5-ylmethoxy)benzyl}-5′-*N*-methylcarbamoyladenosine (CP-608039).[18] These compounds contain the potency- and efficacy-enhancing 5′-methyluronamide moiety and the N^6-hydrophobic moiety. Also, AR agonists that combined N^6-alkyl and 2-alkynyl substitutions proved useful in the identification of A_3 or A_{2B} AR agonists with various selectivity profiles, depending on the type of 2-alkynyl substitution.[19] On the other hand, the truncated nucleosides where the 5′-methyluronamide of the A_3AR agonists was deleted were converted into potent and selective A_3AR antagonists, because there was no 5′-uronamide, which serves as the hydrogen bonding donor required for receptor activation.[20] Among these, compound **1** showed potent antiglaucoma[21] activity (Chart 1).

Chart 1. Design Strategy for Truncated (*N*)-Methanocarba-Nucleosides in This Study[a]

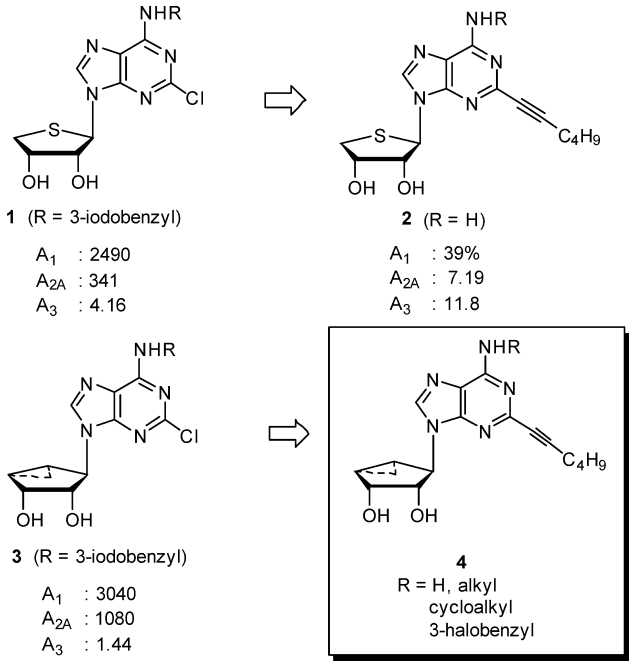

[a] K_i values (nM) or % inhibition at 10 μM in binding to human A_1, A_{2A}, and A_3 adenosine receptors.

Introduction of the 2-hexynyl group on the C2-position of **1** but no substitution on the N^6-position converted **1** into dually acting A_{2A}AR agonist and A_3AR antagonist **2**.[22] Molecular modeling and empirical structure activity studies in both the ribose and the 4′-thioribose series indicated that the C2 binding sites of A_{2A}AR and A_3AR were spacious enough to accommodate the bulky substituent.

Truncated (*N*)-methanocarba-nucleosides **3**[20a] were also reported to be selective and potent A_3AR antagonists, indicating that compound **3** can also serve as a good template for the development of A_3AR ligands. Thus, we designed and synthesized the truncated C2-hexynyl-(*N*)-methanocarba-nucleosides **4**, which hybridize the structure of C2-hexynyl derivative **2** with that of (*N*)-methanocarba-nucleoside **3** to determine if similar biological trends between **2** and **4** were observed. For the synthesis of the target nucleoside **4**, copper-catalyzed[23] and palladium-catalyzed[24] cross-coupling reactions were employed as key steps for functionalization of the C2-position of 6-chloropurine nucleosides. Herein, we report the synthesis of truncated C2-hexynyl-N^6-substituted-(*N*)-methanocarba-nucleosides **4** as potent and selective A_3AR antagonists and their renoprotective effects using TGF-β1-stimulated mProx cells, a cell culture model for kidney fibrosis.[25]

RESULTS AND DISCUSSION

Chemistry. The desired C2-hexynyl-methanocarba-adenosine derivatives **4a**–**4i** were synthesized from our known cyclopentenone intermediate **5**[26] using a palladium-catalyzed cross-coupling reaction as a key step (Scheme 1).

Scheme 1. Synthesis of Truncated (*N*)-Methanocarba-Nucleosides[a]

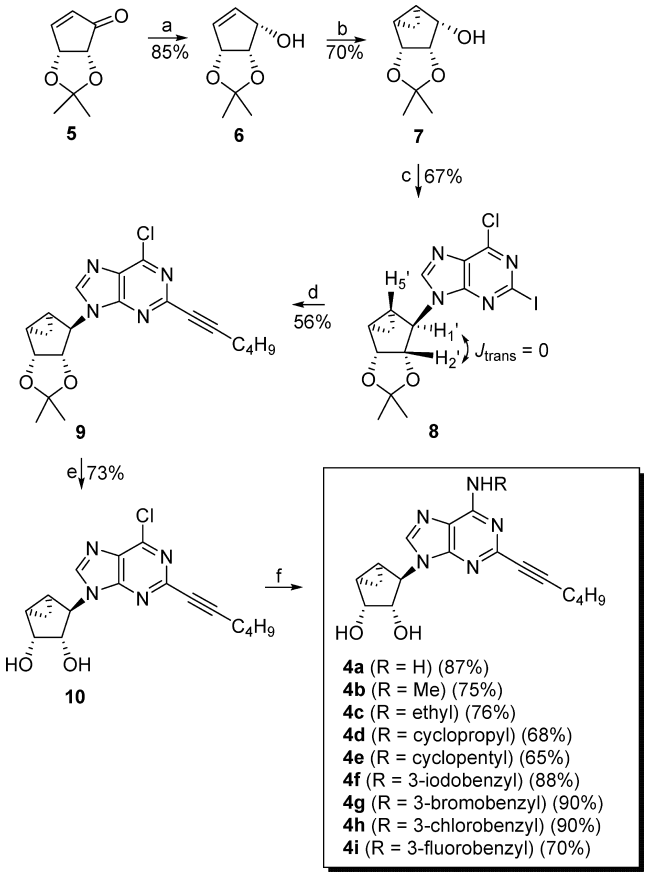

[a] Reagents and conditions: (a) $NaBH_4$, $CeCl_3$–$7H_2O$, methanol, 0 °C, 2 h; (b) Et_2Zn, CH_2I_2, CH_2Cl_2, rt, 5 h; (c) 2-iodo-6-chloropurine, Ph_3P, DIAD, THF, rt, 18 h; (d) 1-hexyne, $(Ph_3P)_4Pd$, Cs_2CO_3, CuI, DMF, 50 °C, 6 h; (e) 2 N HCl/THF (1/1), 40 °C, 18 h; (f) R–NH_2, Et_3N, ethanol, 90 °C, 18 h.

The cyclopentenone derivative **5** was converted to the glycosyl donor **7** according to the reported procedure[27] developed by our laboratory. Direct condensation of **7** with 6-chloro-2-iodopurine[28] under the standard Mitsunobu conditions in THF afforded the β-anomer **8** in 67% yield, similar to a literature report.[29] The anomeric β-configuration of **8** was readily assigned by the diagnostic coupling constants typical of the boat conformation of the bicyclo[3.1.0]hexane system, which has been extensively confirmed by X-ray crystallography

dx.doi.org/10.1021/jm4015313 | J. Med. Chem. 2014, 57, 1344–1354

and NMR analysis.[30] The coupling constants of the $J_{H1',H2'}$ and $J_{H1',H5'}$ should be zero, because both $H_1-C-C-H_2$ and $H_1-C-C-H_5$ dihedral angles with *trans* relationships are close to 90°,[30] indicating that 1′-H of **8** should appear as a singlet. Indeed, ^{1}H NMR of **8** showed that 1′-H appeared as a singlet at 5.03 ppm, confirming the structure of **8**. Sonogashira[31] coupling of **8** with 1-hexyne in the presence of palladium catalyst yielded the C2-hexynyl derivative **9** (56%). Treatment of **9** with 2 N HCl gave the 6-chloro derivative **10**. Substitution of the 6-position of **10** with ammonia and various primary alkyl-, cycloalkyl-, and arylalkyl-amines afforded the final nucleosides **4a**–**4i**.

The target nucleosides were also synthesized using a lithiation-mediated stannyl transfer reaction[28a] and a copper-catalyzed cross-coupling reaction[23] as key steps for functionalization of the C2-position (Scheme 2). The glycosyl donor **7** was condensed with 6-chloropurine under the same conditions used in Scheme 1 to give 6-chloropurine derivative **11**. Treatment of **11** with LiTMP followed by reacting the resulting anion with tri-*n*-butyltin chloride afforded the C2-stannyl derivative **12** exclusively.[28a] Copper-catalyzed coupling[23] of **12** with 1-iodohexyne yielded the 2-hexynyl derivative **9**, which was converted to the same final nucleosides **4a**–**4i** according the same procedure used in Scheme 1.

Scheme 2. Alternative Synthesis of Truncated (*N*)-Methanocarba-Nucleosides[a]

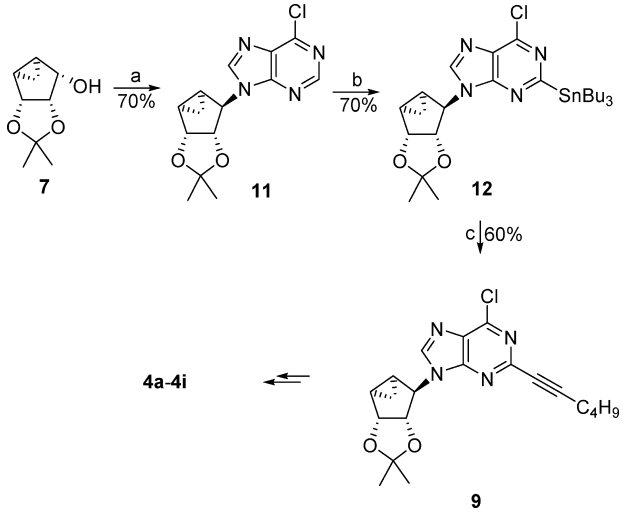

[a]Reagents and conditions: (a) 6-chloropurine, Ph_3P, DIAD, THF, rt, 18 h; (b) LiTMP, Bu_3SnCl, THF, −78 °C, 5 h; (c) 1-iodohexyne, CuI, DMF, 50 °C, 16 h.

Binding Affinity. Binding assays were carried out using standard radioligands and membrane preparations from Chinese hamster ovary (CHO) cells stably expressing the human (h) A_1 or A_3AR, RBL-2H3 basophilic leukemia cells expressing rat (r) A_3AR, or human embryonic kidney (HEK)-293 cells expressing the hA_{2A}AR.[32] Binding at the hA_3AR or rA_3AR in this study was carried out using [^{125}I]N^6-(3-iodo-4-aminobenzyl)-5′-*N*-methylcarboxamidoadenosine (I-AB-MECA, **13**) as a radioligand. Binding at the hA_1AR using [^{3}H] (-)-N^6-2-phenylisopropyl adenosine (R-PIA, **14**) or hA_{2A}AR using [^{3}H]CGS21680 (2-[*p*-(2-carboxyethyl)phenylethylamino]-5′-*N*-ethylcarboxamidoadenosine, **15**) was carried out. In cases of weak binding, the percent inhibition of radioligand binding to the hA_1AR and hA_{2A}AR was determined at 10 μM. Nonspecific binding was defined using 10 μM of 5′-*N*-ethylcarboxamidoadenosine (NECA, **16**).

Because binding affinity of similar (*N*)-methanocarba compounds was reported to be very weak or absent at the hA_{2B}AR subtype,[33] we did not include this receptor in the radioligand binding assays. To confirm that activity of the present chemical series is weak at the A_{2B}AR, we performed a functional assay in CHO cells expressing the hA_{2B}AR. Compound **4b** at 10 μM produced only 15.7 ± 12.6% of the activation of cAMP production seen with full agonist **16**.

As shown in Table 1, a variety of N^6-alkyl, cycloalkyl, and arylalkyl substituents in truncated (*N*)-methanocarba-nucleoside derivatives have produced nanomolar binding affinity at the hA_3AR subtype, indicating that bulky C2 and N^6 substituents could be tolerable in the binding site of A_3AR. However, a hydrophobic substituent at the N^6-position reduced the binding affinity greatly at the hA_{2A} AR subtype in the presence of a hydrophobic C2-hexynyl group, and only an unsubstituted 6-amino group showed good binding affinity (K_i = 100 nM) at the hA_{2A}AR, indicating that the N^6 binding site of hA_{2A}AR is small. This trend is similar to that of truncated 2-hexynyl-4′-thioadenosine (**2**),[22] but truncated carbanucleoside derivative **4a** was 14-fold less potent than truncated 4′-thioadenosine derivative **2**. This result may be due to the fixed conformation of (*N*)-methanocarba-nucleosides unlike the flexible conformation of 4′-thioadenosine derivatives, hindering them from forming a favorable hydrophobic interaction in the binding site of A_{2A}AR. However, all compounds showed very weak binding affinity at the hA_1AR, suggesting that the binding sites may not be large enough to accommodate the bulky C2 and/or N^6 substituent. Among compounds tested, **4b** (R = CH_3) exhibited the highest binding affinity (K_i = 4.9 nM) at the hA_3AR subtype with high selectivity for the hA_1 and hA_{2A}ARs. The primary amine-substituted N^6-alkyl- and N^6-cycloalkyl-derivatives (**4b**–**4e**) generally exhibited better binding affinity at the hA_3AR than the free amino derivative **4a**, except cyclopentyl derivative **4e**. The order of compounds showing high binding affinity at the hA_3AR is as follows: **4b** (R = CH_3, K_i = 4.6 nM) > **4c** (R = ethyl, K_i = 6.7 nM) > **4d** (R = cyclopropyl, K_i = 9.2 nM) > **4a** (R = H, K_i = 16.2 nM). The binding affinities of 3-halobenzylamine derivatives **4f**–**4i** at the hA_3AR did not differ significantly, with K_i values of 7.8–16.0 nM. The binding affinity at the hA_3AR in this series decreased in the following order: 3-Cl derivative **4h**, 3-Br derivative **4g** > 3-I derivative **4f** > 3-F derivative **4i**. All synthesized compounds **4a**–**4i** have also produced nanomolar binding affinity at the rA_3AR, but they showed weaker binding affinity than that at the hA_3AR. The N^6-alkyl derivatives **4b** and **4c** exhibited lower binding affinity at the rA_3AR than the free amino derivative **4a**, the N^6-cycloalkyl derivatives **4d** and **4e**, and the 3-halobenzyl-amine derivatives **4f**–**4i**, which showed similar binding affinities at the rA_3AR, with K_i values in the range of 10.7–65 nM. The 3-chlorobenzyl derivative **4h** exhibited the highest binding affinity (K_i = 10.7 nM) at the rA_3AR, unlike the N^6-methyl derivative **4b** showing the highest affinity (K_i = 4.9 nM) at the hA_3AR.

In a cAMP functional assay[34] at the hA_3AR expressed in CHO cells, the most potent compound **4b** behaved as a partial agonist, in contrast to full antagonists **2** and **3** (Figure 1). Compound **4b** at 10 μM displayed an EC_{50} of 45.8 nM and a maximal stimulation of cAMP formation of 29.1 ± 5.0% relative to the full agonist **16** (= 100%). Similarly, other compounds

dx.doi.org/10.1021/jm4015313 | J. Med. Chem. 2014, 57, 1344–1354

Table 1. Binding Affinities and Anti-Renal Fibrosis Activity of Truncated 2-Hexynyl-N^6-Substituted Derivatives 4a−4i and Reference Nucleosides 2 and 3 at hARs and rA_3AR

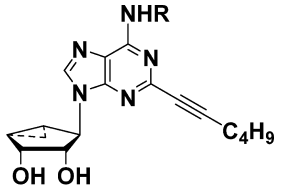

4a-4i

		K_i (nM) or *% inhibition* at 10 μM[a]				
compd no.	R	hA_1AR	$hA_{2A}AR$	hA_3AR	rA_3AR	IC_{50} (μM)[d]
2[b]		*39 ± 10%*	7.19 ± 0.6	11.8 ± 1.3	ND[e]	ND[e]
3[c]		3040 ± 610	1080 ± 310	1.44 ± 0.6	ND[e]	18.6
4a	H	*29% ± 6%*	100 ± 10	16.2 ± 6.7	65 ± 18	6.12
4b	methyl	*14% ± 4%*	7490 ± 590	4.90 ± 1.30	231 ± 81	0.83
4c	ethyl	*31% ± 7%*	2860 ± 1060	6.70 ± 1.80	176 ± 47	0.84
4d	cyclopropyl	2170 ± 510	2200 ± 660	9.20 ± 0.40	39 ± 19	11.8
4e	cyclopentyl	1580 ± 240	1760 ± 410	160 ± 50	58 ± 39	>50
4f	3-iodobenzyl	*48% ± 5%*	2530 ± 170	12.0 ± 6.0	26 ± 22	7.88
4g	3-bromobenzyl	*38% ± 6%*	3150 ± 170	8.60 ± 4.80	59 ± 37	10.4
4h	3-chlorobenzyl	*19% ± 8%*	3310 ± 1220	7.80 ± 1.70	10.7 ± 1.6	2.87
4i	3-fluorobenzyl	*21% ± 4%*	*27% ± 5%*	16.0 ± 10.0	43 ± 30	3.17

[a]All binding experiments were performed using adherent mammalian cells stably transfected with cDNA encoding the appropriate hAR (A_1AR and A_3AR in CHO cells and $A_{2A}AR$ in HEK-293 cells) or rA_3AR expressed endogenously in RBL-2H3 cells. Binding was carried out using 1 nM [^{3}H]**14**, 10 nM [^{3}H]**15**, or 0.5 nM [^{125}I]**13** as radioligands for A_1, A_{2A}, and A_3ARs, respectively. Values expressed as a percentage in italics refer to percent inhibition of specific radioligand binding at 10 μM for 3 − 5 duplicate determinations, with nonspecific binding defined using 10 μM **16**. [b]ref 22. [c]ref 20a. [d]Concentration to inhibit the TGF-β1-induced collagen I mRNA expression by 50%. [e]Not determined.

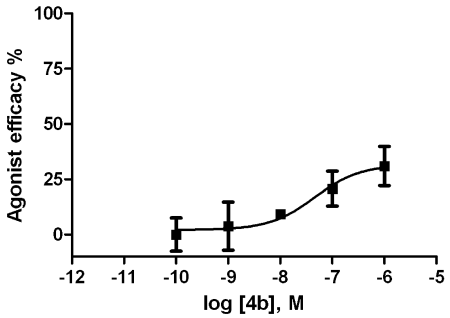

Figure 1. Effect of compound **4b** on forskolin-induced stimulation of cAMP production at the hA_3AR expressed in CHO cells, compared to **16** as reference full agonist (= 100%). A representative curve from three determinations is shown.

proved to be partial agonists of the hA_3AR (% activation relative to **16**, triplicate determination): **4c**, 15.5 ± 6.7; **4d**, 19.8 ± 4.6; **4e**, 27.1 ± 14.6; **4i**, 18.9 ± 7.5. Compounds **4f**, **4g**, and **4h** induced <5% of the activation seen with **16** and were therefore antagonists.

Renoprotective Effects. All synthesized compounds were tested for an antifibrotic effect in murine proximal (mProx) cells, a cell line of mouse proximal tubular epithelial cells.[25] As shown in Table 1, most of the tested compounds strongly inhibited transforming growth factor (TGF)-β1-induced collagen I upregulation. Compound **4b** showed the most potent inhibitory activity (IC_{50} = 0.83 μM) against TGF-β1-induced collagen I mRNA expression (Figure 2). The binding affinity at the A_3AR was almost proportional to the antifibrotic activity, which indicates that the small N^6-hydrophobic substituent is also favored for renoprotective effects.

Molecular Docking Study. The truncated C2-substituted thio-ribose compound **2** (A_{2A} K_i = 7.19 nM) exhibited excellent binding affinity, and the methanocarba analogue **4a** (A_{2A} K_i = 100 nM) showed ≈14-fold less binding affinity at the hA_{2A} AR. In addition, the presence of the 3-iodobenzyl group at the N^6-position in **4f** led to a substantial decrease in its binding affinity at the $hA_{2A}AR$ with a K_i of 2530 nM. In view of the observed variations in the $hA_{2A}AR$ binding affinities among these compounds, molecular docking and binding free energy calculations were carried out considering the X-ray structure of the $hA_{2A}AR$ complexed with an agonist, **16** (PDB code 2YDV[35]). The common interactions among N^6-unsubstituted compounds **2** and **4a** at the $hA_{2A}AR$ includes: (i) the adenine ring stabilized through $\pi-\pi$ stacking interaction with Phe168 (extracellular loop 2) and a H-bonding interaction with Asn253$^{6.55}$, (ii) the exocyclic 6-amino group H-bonded with Asn253$^{6.55}$ and Glu169, and (iii) the projection of C2-hexynyl group toward the extracellular side exhibiting hydrophobic interaction with Phe168, Ile66$^{2.55}$, Leu267$^{7.32}$, Met270$^{7.35}$, Ile274$^{7.39}$, and Tyr271$^{7.36}$ residues (Figure 3).

In contrast, they exhibited different binding modes at the ribose binding site formed by Val84$^{3.32}$, Leu85$^{3.33}$, Trp246$^{6.48}$, Leu249$^{6.51}$ and Ile274$^{7.39}$, Ser277$^{7.42}$, and His278$^{7.43}$. The 2′- and 3′-hydroxyl groups of **2** formed H-bonds with the two key residues His278$^{7.43}$ and Ser277$^{7.42}$, respectively (Figure 3A), whereas **4a** lost one of the key H-bond interactions with Ser277$^{7.42}$ (Figure 3B). This residue Ser277 is a key residue reported to be important for $hA_{2A}AR$ agonistic activity and potency using site-directed mutagenesis.[36−38] It appears that a decrease in the binding affinity of **4a** at the $hA_{2A}AR$ could be due to the loss of H-bonding with Ser277$^{7.42}$ at the ribose binding site. The loss of H-bonding with Ser277$^{7.42}$ may particularly be attributed to the methanocarba ring (**4a**), being

dx.doi.org/10.1021/jm4015313 | J. Med. Chem. 2014, 57, 1344−1354

4b (μM)	*COL1A1* Gene expression, Mean±SE[a]	% of inhibition[b]
Control (no TGF-β1)	0.195±0.035	100
0	1.00	0
1	0.532±0.022	57.4
10	0.447±0.01	67.9
20	0.383±0.041	75.7
50	0.241±0.004	93.1
IC_{50}	0.83 μM	

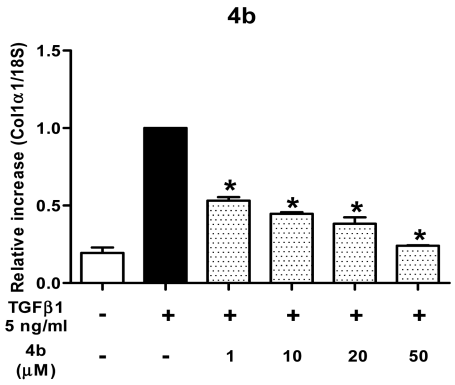

Figure 2. Inhibition of TGF-β1-induced *COL1A1* gene expression in mProx24 cells, a cell line of mouse proximal tubular epithelial cells, by **4b**. Data are mean ± SE of three experiments. *$p < 0.05$ vs TGF-β1-stimulated mProx24 cells: [a]relative increase in *COL1A1* gene expression (1.0 is the effect of 5 ng/mL TGF-β1), [b]at the concentration of **4b** in μM indicated in column 1.

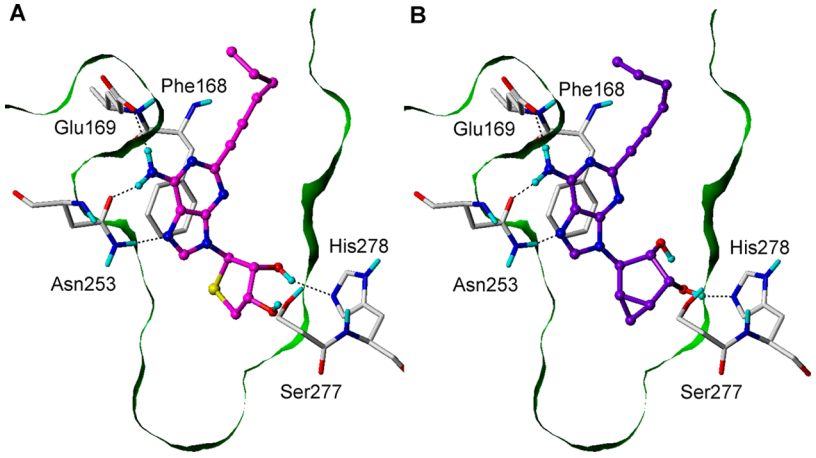

Figure 3. Predicted binding modes of N^6-unsubstituted nucleosides **2** (A) and **4a** (B) in the $hA_{2A}AR$ agonist-bound crystal structure. Compounds **2** and **4a** are depicted in ball-and-stick, with carbon atoms in magenta and purple, respectively. The key amino acid residues are shown as capped-stick, with carbon atoms in white. The Connolly surface of the receptor was generated by MOLCAD with green color and z-clipped for visual convenience. The hydrogen bonds are shown as black dashed lines, and the nonpolar hydrogen atoms are not displayed for clarity.

less flexible than the thio-ribose ring (**2**). Furthermore, the calculated prime MM-GBSA binding free energies (ΔG_{bind}) for **2** and **4a** were −104.16 and −90.37 kcal/mol, respectively, which are in good agreement with their observed binding affinities at the $hA_{2A}AR$. However, **4f** with a bulky group at the N^6-position did not fit well at the binding site of the hA_{2A} AR. These results show that the H-bond interactions with both $Ser277^{7.42}$ and $His278^{7.43}$ at the ribose binding site are important for high affinity and potency, and the bulky group at the N^6-position is unfavorable toward high binding affinity at the $hA_{2A}AR$.

In addition, we also performed the molecular docking studies of the analogues **2** and **4a** to hA_3AR (see Figure 1S in Supporting Information). Because the X-ray crystal structure of hA_3AR is not available yet, the homology model available in the Protein Data Bank (PDB code 1OEA) was used. The docking results showed that the binding modes of the analogues in hA_3AR are flipped compared to those in $hA_{2A}AR$. In hA_3AR, the bulky C2-hexynyl group positions toward the middle of the trans-membrane region exhibited hydrophobic interactions. However, in $hA_{2A}AR$, there is limited space at the bottom of the pocket, making the bulky hexynyl group face toward the extracellular side. The NH_2 group at N^6-position forms the hydrogen bonding with Asn6.55 in both $hA_{2A}AR$ (Asn253) and hA_3AR (Asn250). Interestingly, there is a relatively bigger space near this region in hA_3AR, whereas the NH_2 group binds tightly in the pocket of $hA_{2A}AR$. It appears according to this docking mode that this is why the N^6-substituted derivatives (**4b**−**4i**) maintained their binding affinity at the hA_3AR, but not at the $hA_{2A}AR$.

CONCLUSIONS

The series of truncated N^6-substituted-(*N*)-methanocarba-adenosine derivatives, **4a**−**4i** with 2-hexynyl group were synthesized in order to examine if this class of nucleosides behaves as the corresponding 4′-thioadenosine derivatives. The functionalization at the C2-position of 6-chloropurine derivatives was achieved using lithiation-mediated stannyl transfer and copper- or palladium-catalyzed cross-coupling reactions. It was revealed that all synthesized nucleosides showed very high binding affinity at the hA_3AR as well as at the rA_3AR, as in the case of the corresponding 4′-thioadenosine derivatives, indicating that the hydrophobic N^6 and/or C2 substituent could be tolerable in the binding site of the A_3AR. However,

dx.doi.org/10.1021/jm4015313 | J. Med. Chem. 2014, 57, 1344−1354

only an unsubstituted 6-amino group in the presence of a bulky C2-hexynyl group was associated with high binding affinity at the $hA_{2A}AR$ (compound **4a**). This trend is similar to that of the corresponding 4′-thioadenosine derivatives, serving as dual acting A_{2A} and A_3AR ligands. However, the binding affinity at the $hA_{2A}AR$ of the truncated (*N*)-methanocarba-nucleoside **4a** is 14-fold less potent than the truncated 4′-thioadenosine derivative **2**. It is attributed to the loss of key hydrogen bonding due to the rigid structure, which was confirmed by a $hA_{2A}AR$ molecular docking study.

The specific structure−activity relationship for this series of conformationally constrained nucleosides might arise from the molecule of lacking in the flexibility required for optimal interaction in the binding site because of the rigidity of (*N*)-methanocarba-nucleosides. From this study, N^6-methyl derivative **4b** was discovered as a preferred hA_3AR ligand (low efficacy partial agonist) with high selectivity, whereas 3-chlorobenzyl derivative **4h** was discovered as the most potent/selective rA_3AR ligand in this series.

The nature of the N^6 substituent in this chemical series modulates the level of hA_3AR agonist efficacy (ranging from nearly 0% to 29% of full agonist). For these assays, we used a CHO cell with a high level of stable expression of the hA_3AR, which would tend to amplify partial agonist action. Because even these partial agonists have a relatively low efficacy, they can be expected to behave similarly to full antagonists in some pharmacological models, especially in cases of low receptor expression.[39]

A_3AR antagonist **1** was recently shown to inhibit unilateral ureteral obstruction-induced renal fibrosis and collagen I upregulation.[40] This suggests that A_3AR antagonists might be useful therapeutically to block the development and attenuate the progression of renal fibrosis. All of the compounds synthesized here were screened for renoprotective activity. Among compounds tested, **4b** exhibited the most potent inhibitory activity (IC_{50} = 0.83 μM) against TGF-β1-induced collagen I upregulation. These findings indicate that this series of truncated (*N*)-methanocarba-nucleoside derivatives acting as partial agonists of low efficacy or as antagonists, which show high binding affinity at the human A_3AR, can serve as a good lead for the development of antirenal fibrosis agents.

EXPERIMENTAL SECTION

Chemical Synthesis. *General Methods.* ^{1}H NMR spectra ($CDCl_3$, CD_3OD, or DMSO-d_6) were recorded on a Varian Unity Invoa 400 MHz instrument. The ^{1}H NMR data are reported as peak multiplicities: s for singlet, d for doublet, dd for doublet of doublets, t for triplet, q for quartet, brs for broad singlet, and m for multiplet. Coupling constants are reported in hertz. ^{13}C NMR spectra ($CDCl_3$, CD_3OD, or DMSO-d_6) were recorded on a Varian Unity Inova 100 MHz instrument. ^{19}F NMR spectra ($CDCl_3$, CD_3OD) were recorded on a Varian Unity Inova 376 MHz instrument. The chemical shifts were reported as parts per million (δ) relative to the solvent peak. Optical rotations were determined on Jasco III in appropriate solvent. UV spectra were recorded on U-3000 made by Hitachi in methanol or water. Infrared spectra were recorded on FT-IR (FTS-135) made by Bio-Rad. Melting points were determined on a Buchan B-540 instrument and are uncorrected. Elemental analyses (C, H, and N) were used to determine the purity of all synthesized compounds, and the results were within ±0.4% of the calculated values, confirming ≥95% purity. Reactions were checked with TLC (Merck precoated 60F254 plates). Flash column chromatography was performed on silica gel 60 (230−400 mesh, Merck). Reagents were purchased from Aldrich Chemical Co. Solvents were obtained from local suppliers. All the anhydrous solvents used were redistilled over CaH, P_2O_5 or sodium/benzophenone prior to the reaction.

*6-Chloro-9-((3aR,3bR,4aS,5R,5aS)-hexahydro-2,2dimethyl-bicyclo[3.1.0]hex-1(5)-eno[3,2-d] [1,3]dioxol-5-yl)-2-iodo-9H-purine (**8**).* To a stirred solution of 2-iodo-6-chloropurine (1.23 g, 4.4 mmol) and triphenylphosphine (Ph_3P) (1.90 g, 4.4 mmol) in anhydrous THF (20 mL) was added diisopropyl azodicarboxylate (DIAD) (1.44 mL, 9.16 mmol) in THF (10 mL) under N_2 at 0 °C, and the mixture was stirred at the same temperature for 15 min. To this solution was added a solution of compound **7**[19] (0.5 g, 2.93 mmol) in THF (10 mL) at 0 °C, and the reaction mixture was stirred at room temperature for 16 h. The reaction mixture was concentrated under reduced pressure, and the crude residue was purified by flash silica gel column chromatography (hexane: EtOAc = 3:1) to give **8** (0.85 g, 67%) as a white solid: mp 94−96 °C; UV (MeOH) λ_{max} 282 nm. MS (ESI): $[M + H]^+$ calcd for $C_{14}H_{15}ClIN_4O_2$, 432.9923; found, 432.9931; $[\alpha]^{25}_D$ = −10.4 (*c* 0.2, MeOH); ^{1}H NMR ($CDCl_3$) δ 0.95−1.01 (m, 2 H), 1.26 (s, 3 H), 1.55 (s, 3 H), 1.63−1.68 (m, 1 H), 2.12−2.18 (m, 1 H), 4.65−4.68 (m, 1 H), 5.03 (s, 1 H), 5.35−5.38 (m, 1 H), 8.12 (s, 1 H); ^{13}C NMR ($CDCl_3$) δ 9.4, 24.4, 25.6, 26.1, 26.5, 61.5, 81.6, 89.1, 112.8, 116.9, 132.1, 143.9, 150.9, 152.1. Anal. ($C_{14}H_{14}ClIN_4O_2$) C, H, N.

*6-Chloro-2-(hex-1-ynyl)-9-((3aR,3bR,4aS,5R,5aS)-hexahydro-2,2-dimethylbicyclo [3.1.0]hex-1(5)-eno[3,2-d][1,3]dioxol-5-yl)-9H-purine (**9**).* To a stirred solution of **8** (0.30 g, 0.69 mmol) in anhydrous DMF (10 mL) were added tetrakis(triphenylphosphine)palladium ($(Ph_3P)_4Pd$) (0.20 g, 0.17 mmol), copper iodide (0.016 g, 0.08 mmol), cesium carbonate (0.226 g, 0.69 mmol), and 1-hexyne (0.07 mL, 0.62 mmol) at room temperature and the reaction mixture was stirred at 50 °C for 5 h. The reaction mixture was cooled to room temperature, quenched with saturated $NaHCO_3$ (5 mL) solution, and diluted with EtOAc (10 mL). The organic layer was separated and aqueous layer was further extracted with EtOAc (3 × 5 mL). The combined organic layers were washed with brine (10 mL) and water (10 mL), dried over anhydrous $MgSO_4$, and filtered. The solvent was evaporated under reduced pressure and the crude residue was purified by flash silica gel column chromatography (hexane: EtOAc = 3:1) to give **9** (0.15 g, 56%) as a white foam: mp 105−107 °C; UV (MeOH) λ_{max} 284 nm. MS (ESI^+): $[M + H]^+$ calcd for $C_{20}H_{24}ClIN_4O_2$, 387.1582; found, 387.1586; $[\alpha]^{25}_D$ = +2.5 (*c* 0.2, MeOH). ^{1}H NMR ($CDCl_3$, 400 MHz) δ: 0.94−1.03 (m, 5 H), 1.25 (s, 3 H), 1.47−1.54 (m, 2 H), 1.55 (s, 3 H), 1.63−1.70 (m, 3 H), 2.12−2.17 (m, 1 H), 2.48−2.51 (t, 2 H, *J* = 7.2 Hz), 4.63−4.65 (d, 1 H, *J* = 5.1 Hz), 5.13 (s, 1 H), 5.35−5.38 (t, 1 H, *J* = 6.00 Hz), 8.13 (s, 1 H). ^{13}C NMR ($CDCl_3$, 100 MHz) δ: 9.3, 13.7, 19.2, 22.3, 24.4, 25.3, 26.0, 26.5, 30.2, 60.7, 79.7, 81.4, 89.1, 90.9, 112.6, 130.8, 144.2, 146.3, 151.1, 151.3. Anal. ($C_{20}H_{23}ClIN_4O_2$) C, H, N.

*(1R,2R,3S,4R,5S)-4-(6-Chloro-2-(hex-1-ynyl)-9H-purin-9yl)bicyclo-[3.1.0]hexane-2,3-diol (**10**).* To a stirred ice-cooled solution of **9** (0.30 g, 0.77 mmol) in THF (3 mL) was added 2 N HCl (3 mL), and the mixture was stirred at 40 °C for 16 h. The reaction mixture was neutralized with saturated $NaHCO_3$ (2 mL) solution and then diluted with EtOAc (10 mL). The organic layer was separated, and the aqueous layer was further extracted with EtOAc (2 × 5 mL). The combined organic layers were washed with brine (10 mL), dried over anhydrous $MgSO_4$, filtered, and evaporated under reduced pressure. The crude residue was purified by flash silica gel column chromatography (hexane: EtOAc = 2:1) to give **10** (0.22 g, 73%) as a white solid: mp 120−122 °C; UV (MeOH) λ_{max} 285 nm. MS (ESI^+): $[M + H]^+$ calcd for $C_{17}H_{20}ClN_4O_2$, 347.1269; found, 347.1274; $[\alpha]^{25}_D$ = +27.0 (*c* 0.2, MeOH). ^{1}H NMR ($CDCl_3$, 400 MHz) δ: 0.84−0.87 (m, 1 H), 0.94−0.97 (t, 3 H, *J* = 7.2 Hz), 1.29−1.32 (m, 1 H), 1.47−1.53 (m, 2 H), 1.62−1.70 (m, 3 H), 2.10−2.14 (m, 1 H), 2.47−2.51 (t, 2 H, *J* = 7.2 Hz), 4.05−4.06 (d, 1 H, *J* = 6.0 Hz), 4.86−4.89 (t, 1 H, *J* = 6.0 Hz), 5.04 (s, 1 H), 8.20 (s, 1 H). ^{13}C NMR ($CDCl_3$, 100 MHz) δ: 7.8, 14.1, 19.6, 19.9, 22.7, 24.6, 30.6, 63.4, 72.3, 77.1, 79.9, 91.8, 131.3, 144.4, 146.5, 151.6, 151.7. Anal. ($C_{17}H_{19}ClN_4O_2$) C, H, N.

*(1R,2R,3S,4R,5S)-4-(6-Amino-2-(hex-1-ynyl)-9H-purin-9-yl)-bicyclo[3.1.0]hexane-2, 3-diol (**4a**).* A solution of **10** (0.05 g, 0.42 mmol) in saturated NH_3 in *t*-BuOH (5 mL) was stirred at 110 °C for

dx.doi.org/10.1021/jm4015313 | J. Med. Chem. 2014, 57, 1344−1354

16 h. The reaction mixture was evaporated, and the residue was purified by flash silica gel column chromatography (CH_2Cl_2: MeOH = 9: 1) to give **4a** (0.103 g, 87%) as a white solid: mp 122−124 °C; UV (MeOH) λ_{max} 271 nm. MS (ESI^+): $[M + H]^+$ calcd for $C_{17}H_{22}N_5O_2$, 329.1796; found, 329.1797; $[\alpha]^{25}_D$ = +14.7 (*c* 1.75, MeOH). ^1H NMR (CD_3OD, 400 MHz) *δ*: 0.76−0.78 (m, 1 H), 0.96−1.00 (t, 3 H, *J* = 7.2 Hz), 1.34−1.37 (m, 1 H), 1.50−1.70 (m, 5 H), 1.98−2.01 (m, 1 H), 2.45−2.48 (t, 2 H, *J* = 7.2 Hz), 3.86−3.88 (d, 1 H, *J* = 6.8 Hz), 4.66−4.69 (t, 1 H, *J* = 5.6 Hz), 4.83 (s, 1 H), 8.24 (s, 1 H). ^{13}C NMR (CD_3OD) *δ*: 8.2, 14.1, 19.6, 19.7, 23.2, 24.7, 31.6, 64.0, 73.0, 77.4, 81.3, 88.6, 120.3, 141.4, 147.9, 157.2, 167.2. Anal. ($C_{17}H_{21}N_5O_2$) C, H, N.

*General Procedure for the Synthesis of **4b**−**4i**.* To a solution of **10** (1 equiv) in EtOH (10 mL) were added Et_3N (3 equiv) and the appropriate amine (1.5 equiv) at room temperature, and the mixture was stirred at 90 °C for 18 h in a steel bomb. The reaction mixture was evaporated and the residue was purified by flash silica gel column chromatography (CH_2Cl_2/MeOH = 12:1) to give **4b**−**4i**.

*(1R,2R,3S,4R,5S)-4-(2-(Hex-1-ynyl)-6-(methylamino)-9H-purin-9-bicyclo[3.1.0]hexane-2,3-diol (**4b**).* Yield: 75%; white solid; mp 118−120 °C; UV (MeOH) λ_{max} 273 nm. MS (ESI^+): $[M + H]^+$ calcd for $C_{18}H_{24}N_5O_2$, 342.1925; found, 342.1925; $[\alpha]^{25}_D$ = +35.5 (*c* 0.2, MeOH). ^1H NMR (CD_3OD, 400 MHz) *δ*: 0.73−0.79 (m, 1 H), 0.96−1.00 (t, 3 H, *J* = 7.2 Hz), 1.34−1.38 (m, 1 H), 1.49−1.71 (m, 5 H), 1.95−2.01 (m, 1 H), 2.45−2.49 (t, 2 H, *J* = 7.2 Hz), 3.11 (brs, 3 H), 3.84−3.86 (d, 1 H, *J* = 6.8 Hz), 4.64−4.67 (t, 1 H, *J* = 5.6 Hz), 4.82 (s, 1 H), 8.16 (s, 1 H). ^{13}C NMR (CD_3OD, 100 MHz) *δ*: 7.9, 13.9, 19.6, 19.6, 23.2, 24.6, 27.8, 31.6, 63.8, 73.0, 77.2, 81.6, 87.9, 120.2, 140.3, 148.1, 149.4, 156.6. Anal. ($C_{18}H_{23}N_5O_2$) C, H, N.

*(1R,2R,3S,4R,5S)-4-(6-(ethylamino)-2-(hex-1-ynyl)-9H-purin-9-yl)-bicyclo[3.1.0]hexane-2,3-diol (**4c**).* Yield: 76%; white solid; mp 98−100 °C; UV (MeOH) λ_{max} 273 nm. MS (ESI^+): $[M + H]^+$ calcd for $C_{19}H_{26}N_5O_2$, 356.2081; found, 356.2083; $[\alpha]^{25}_D$ = +8.5 (*c* 0.2, MeOH); ^1H NMR (CD_3OD, 400 MHz) *δ*: 0.74−0.77 (m, 1 H), 0.96−1.00 (t, 3 H, *J* = 7.2 Hz), 1.27−1.31 (t, 3 H, *J* = 7.2 Hz), 1.34−1.37 (m, 1 H), 1.50−1.70 (m, 5 H), 1.96−2.00 (m, 1 H), 2.45−2.50 (t, 2 H, *J* = 7.2 Hz), 3.62 (brs, 2 H), 3.84−3.85 (d, 1 H, *J* = 6.8 Hz), 4.64−4.67 (t, 1 H, *J* = 5.6 Hz), 4.81 (s, 1 H), 8.16 (s, 1 H). ^{13}C NMR (CD_3OD, 100 MHz) *δ*: 7.9, 14.0, 15.1, 19.5, 19.2, 23.2, 24.6, 31.6, 36.6, 63.8, 73.1, 77.1, 81.6, 87.9, 119.9, 140.3, 148.1, 149.5, 155.9. Anal. ($C_{19}H_{25}N_5O_2$) C, H, N.

*(1R,2R,3S,4R,5S)-4-(6-(Cyclopropylamino)-2-(hex-1-ynyl)-9H-purin-9-yl)bicyclo[3.1.0]hexane-2,3-diol (**4d**).* Yield: 68%; white solid; mp 94−96 °C; UV (MeOH) λ_{max} 275.0 nm. MS (ESI^+): $[M + H]^+$ calcd for $C_{20}H_{26}N_5O_2$, 356.2081; found, 368.2078; $[\alpha]^{25}_D$ = +20.2 (*c* 0.2, MeOH). ^1H NMR (CD_3OD, 400 MHz) *δ*: 0.61−0.65 (m, 2 H), 0.73−0.79 (m, 1 H), 0.86−0.91 (m, 2 H), 0.96−1.00 (t, 3 H, *J* = 7.2 Hz), 1.33−1.38 (m, 1 H), 1.48−1.71 (m, 5 H), 1.95−2.01 (m, 1 H), 2.46−2.50 (t, 2 H, *J* = 7.2 Hz), 3.05 (brs, 1 H), 3.84−3.86 (d, 1 H, *J* = 6.8 Hz), 4.65−4.67 (t, 1 H, *J* = 5.6 Hz), 4.83 (s, 1 H), 8.18 (s, 1 H). ^{13}C NMR (CD_3OD, 100 MHz) *δ*: 7.7, 7.9, 14.0, 19.6, 19.7, 23.2, 24.6, 24.8, 31.6, 63.8, 73.0, 77.2, 81.6, 88.2, 120.1, 140.7, 148.0, 149.8, 157.1. Anal. ($C_{20}H_{25}N_5O_2$) C, H, N.

*(1R,2R,3S,4R,5S)-4-(6-(Cyclopentylamino)-2-(hex-1-ynyl)-9H-purin-9-yl)bicyclo[3.1.0]hexane-2,3-diol (**4e**).* Yield: 65%; white solid; mp 95−97 °C; UV (MeOH) λ_{max} 275 nm. MS (ESI^+): $[M+H]^+$ calcd for $C_{22}H_{30}N_5O_2$, 396.2394; found, 396.2400; $[\alpha]^{25}_D$ = +21.4 (*c* 0.2, MeOH). ^1H NMR (CD_3OD, 400 MHz) *δ*: 0.74−0.78 (m, 1 H), 0.96−1.00 (t, 3 H, *J* = 7.2 Hz), 1.34−1.37 (m, 1 H), 1.50−1.83 (m, 10 H), 1.96−1.99 (m, 2 H), 2.06−2.12 (m, 2 H), 2.45−2.48 (t, 2 H, *J* = 7.2 Hz), 3.83−3.85 (d, 1 H, *J* = 6.4 Hz), 4.60 (brs, 1 H), 4.64−4.67 (t, 1 H, *J* = 5.6 Hz), 4.81(s, 1 H), 8.18 (s, 1 H). ^{13}C NMR (CD_3OD, 100 MHz) *δ*: 7.9, 13.9, 19.55, 19.60, 23.2, 24.6, 24.7, 31.6, 34.0, 53.5, 63.8, 73.0, 77.1, 81.7, 87.9, 119.8, 140.3, 148.1, 149.5, 155.5. Anal. ($C_{22}H_{29}N_5O_2$) C, H, N.

*(1R,2R,3S,4R,5S)-4-(6-(3-Iodobenzylamino)-2-(hex-1-ynyl)-9H-purin-9-yl)bicyclo[3.1.0]hexane-2,3-diol (**4f**).* Yield: 88%; white solid; mp 128−130 °C; UV (MeOH) λ_{max} 274 nm. MS (ESI^+): $[M + H]^+$ calcd for $C_{24}H_{27}IN_5O_2$, 544.1204; found, 544.1212; $[\alpha]^{25}_D$ = +30.3 (*c* 0.2, MeOH). ^1H NMR (CD_3OD, 400 MHz) *δ*: 0.73−0.79 (m, 1 H), 0.96−1.00 (t, 3 H, *J* = 7.2 Hz), 1.34−1.37 (m, 1 H), 1.50−1.58 (m, 2 H), 1.60−1.72 (m, 3 H), 1.96−2.01 (m, 1 H), 2.45−2.48 (t, 2 H, *J* = 7.2 Hz), 3.85−3.87 (d, 1 H, *J* = 6.4 Hz), 4.65−4.67 (t, 1 H, *J* = 5.6 Hz), 4.76 (brs, 2 H), 4.83 (s, 1 H), 7.07−7.11 (t, 1 H, *J* = 7.6 Hz), 7.39−7.41 (m, 1 H), 7.59−7.61 (m, 1 H), 7.80 (s, 1 H), 8.19 (s, 1 H). ^{13}C NMR (CD_3OD, 100 MHz) *δ*: 7.9, 14.0, 19.5, 19.6, 23.2, 24.6, 31.6, 44.4, 63.8, 73.1, 77.1, 81.7, 88.1, 94.9, 120.1, 128.2, 131.4, 137.4, 137.9, 140.7, 143.1, 147.9, 149.9, 155.7. Anal. ($C_{24}H_{26}IN_5O_2$) C, H, N.

*(1R,2R,3S,4R,5S)-4-(6-(3-Bromobenzylamino)-2-(hex-1-ynyl)-9H-purin-9-yl)bicyclo[3.1.0]hexane-2,3-diol (**4g**).* Yield: 90%; white solid; mp 124−126 °C; UV (MeOH) λ_{max} 275 nm. MS (ESI^+): $[M + H]^+$ calcd for $C_{24}H_{27}BrN_5O_2$, 496.1343; found, 496.1350; $[\alpha]^{25}_D$ = +21.2 (*c* 0.2, MeOH). ^1H NMR (CD_3OD, 400 MHz) *δ*: 0.75−0.77 (m, 1 H), 0.96−1.00 (t, 3 H, *J* = 7.2 Hz), 1.34−1.37 (m, 1 H), 1.50−1.56 (m, 2 H), 1.60−1.71 (m, 3 H), 1.97−1.99 (m, 1 H), 2.45−2.48 (t, 2 H, *J* = 7.2 Hz), 3.85−3.87 (d, 1 H, *J* = 6.8 Hz), 4.65−4.68 (t, 1 H, *J* = 5.6 Hz), 4.80 (brs, 2 H), 4.83 (s, 1 H), 7.22−7.26 (m, 1 H), 7.36−7.41 (m, 2 H), 7.59 (s, 1 H), 8.19 (s, 1 H). ^{13}C NMR (CD_3OD, 100 MHz) *δ*: 7.9, 14.0, 19.2, 19.6, 23.2, 24.6, 31.6, 44.5, 63.9, 73.1, 77.2, 81.6, 88.0, 120.1, 123.5, 127.6, 131.3, 131.4, 131.8, 140.7, 143.2, 148.0, 150.0, 155.8. Anal. ($C_{24}H_{26}BrN_5O_2$) C, H, N.

*(1R,2R,3S,4R,5S)-4-(6-(3-Chlorobenzylamino)-2-(hex-1-ynyl)-9H-purin-9-yl)bicyclo[3.1.0] hexane-2,3-diol (**4h**).* Yield: 90%; white solid; mp 109−111 °C; UV (MeOH) λ_{max} 274 nm. MS (ESI^+): $[M + H]^+$ calcd for $C_{24}H_{27}ClN_5O_2$, 452.1848; found, 452.1842; $[\alpha]^{25}_D$ = +13.1 (*c* 0.2, MeOH). ^1H NMR (CD_3OD, 400 MHz) *δ*: 0.73−0.79 (m, 1 H), 0.90−1.00 (t, 3 H, *J* = 7.2 Hz), 1.34−1.37 (m, 1 H), 1.50−1.72 (m, 5 H), 1.96−2.04 (m, 1 H), 2.44−2.48 (t, 2 H, *J* = 7.2 Hz), 3.85−3.87 (d, 1 H, *J* = 6.8 Hz), 4.65−4.68 (t, 1 H, *J* = 5.6 Hz), 4.80 (brs, 2 H), 4.83 (s, 1 H), 7.24−7.34 (m, 3 H), 7.42−7.43 (m, 1 H), 8.19 (s, 1 H). ^{13}C NMR (CD_3OD, 100 MHz) *δ*: 7.9, 14.0, 19.5, 19.6, 23.1, 24.6, 31.6, 44.6, 63.8, 73.0, 77.1, 81.7, 88.1, 120.5, 127.1, 128.3, 128.8, 131.1, 135.4, 140.7, 142.9, 147.9, 149.9, 155.8. Anal. ($C_{24}H_{26}ClN_5O_2$) C, H, N.

*(1R,2R,3S,4R,5S)-4-(6-(3-Fluorobenzylamino)-2-(hex-1-ynyl)-9H-purin-9-yl)bicyclo[3.1.0] hexane-2,3-diol (**4i**).* Yield: 70%; white solid; mp 99−101 °C; UV (MeOH) λ_{max} 273 nm. MS (ESI^+): $[M + H]^+$ calcd for $C_{24}H_{27}FN_5O_2$, 436.2143; found, 436.2141; $[\alpha]^{25}_D$ = +2.5 (*c* 0.2, MeOH). ^1H NMR (CD_3OD, 400 MHz) *δ*: 0.73−0.79 (m, 1 H), 0.96−1.00 (t, 3 H, *J* = 7.2 Hz), 1.35−1.37 (m, 1 H), 1.49−1.71 (m, 5 H), 1.95−2.01 (m, 1 H), 2.44−2.47 (t, 2 H, *J* = 7.2 Hz), 3.85−3.87 (d, 1 H, *J* = 6.4 Hz), 4.65−4.67 (t, 1 H, *J* = 5.6 Hz), 4.80 (brs, 2 H), 4.83 (s, 1 H), 6.94−6.99 (m, 1 H), 7.12−7.15 (m, 1 H), 7.20−7.22 (m, 1 H), 7.30−7.35 (m, 1 H), 8.18 (s, 1 H). ^{13}C NMR (CD_3OD, 100 MHz) *δ*: 7.9, 13.9, 19.5, 19.6, 23.1, 24.6, 31.6, 44.6, 63.8, 73.0, 77.1, 81.7, 88.0, 115.3, 115.5, 120.0, 124.5, 131.2, 131.3, 140.7, 143.5, 148.0, 150.0, 155.8. Anal. ($C_{24}H_{26}FN_5O_2$) C, H, N.

*6-Chloro-9-((3aR,3bR,4aS,5R,5aS)-Hexahydro-2,2-dimethylbicyclo[3.1.0]hex-1(5)-eno [3,2-d][1,3] dioxol-5-yl)-9H-purine (**11**).* Compound **6** (0.50 g, 2.93 mmol) was converted to **11** (0.63 g, 70%) as a white solid according to the same procedure used in the preparation of **8**: mp 84−86 °C; UV(CH_2Cl_2) λ_{max} 265 nm. MS (ESI^+): $[M + H]^+$ calcd for $C_{14}H_{16}ClN_4O_2$, 307.0956; found, 307.0951; $[\alpha]^{25}_D$ = −40.5 (*c* 0.2, MeOH). ^1H NMR ($CDCl_3$, 400 MHz) *δ*: 0.96−1.04 (m, 2 H), 1.24 (s, 3 H), 1.56 (s, 3 H), 1.70−1.75 (m, 1 H), 2.13−2.19 (m, 1 H), 4.68−4.70 (m, 1 H), 5.08 (s, 1 H), 5.36−5.39 (t, 1 H, *J* = 6.8 Hz), 8.18 (s, 1 H), 8.78 (s, 1 H). ^{13}C NMR ($CDCl_3$, 100 MHz) *δ*: 9.3, 24.3, 25.5, 26.0, 26.1, 61.4, 81.4, 89.1, 112.6, 132.1, 143.9, 151.3, 151.4, 152.3. Anal. ($C_{14}H_{15}ClN_4O_2$) C, H, N.

*2-(Tributylstannyl)-6-chloro-9-((3aR,3bR,4aS,5R,5aS)-hexahydro-2,2-dimethylbicyclo[3.1.0] hex-1(5)-eno[3,2-d][1,3]dioxol-5-yl)-9H-purine (**12**).* To a stirred solution of 2,2,6,6-tetramethylpiperidine (TMP, 1.36 mL, 8.00 mmol) in dry hexane (5 mL) and dry THF (10 mL) was added *n*-butyllithium (5.6 mL, 1.5 M solution in hexanes, 8.47 mmol) dropwise at −78 °C over 30 min, and the mixture was stirred at the same temperature for 1 h. To this mixture, a solution of **11** (0.50 g, 1.60 mmol) in dry THF (10 mL) was added dropwise, and the mixture was stirred at −78 °C for 30 min. Tributyltin chloride (1.74 mL, 8.0 mmol) was successively added dropwise to the dark

dx.doi.org/10.1021/jm4015313 | J. Med. Chem. 2014, 57, 1344−1354

reaction mixture, and the mixture was stirred at the same temperature for another 2 h. The resulting dark solution was quenched by dropwise addition of a saturated aqueous NH_4Cl solution (15 mL). After the mixture was stirred at room temperature for 15 h, the mixture was diluted with CH_2Cl_2 (15 mL). The organic layer was washed with saturated $NaHCO_3$ solution, dried over anhydrous $MgSO_4$, and filtered. The solvent was evaporated under reduced pressure. The crude syrup was purified by flash silica gel column chromatography (hexane/EtOAc = 5:1) to give **12** (0.68 g, 70%) as a colorless syrup: UV (MeOH) λ_{max} 269 nm. MS (ESI^+): $[M + H]^+$ calcd for $C_{26}H_{42}ClN_4O_2Sn$, 597.2011; found, 595.2020; $[\alpha]^{25}_D = -36.5$ (*c* 0.2, MeOH). ^1H NMR ($CDCl_3$) δ: 0.85−0.97 (m, 11 H), 1.13−1.38 (m, 15 H), 1.52−1.67 (m, 10 H), 2.03−2.13(m, 1 H), 4.79−4.81 (d, 1 H, *J* = 7.2 Hz), 4.96 (s, 1 H), 5.43- 5.47 (m, 1 H), 8.01 (s, 1 H). ^{13}C NMR (CD_3OD) δ: 9.4, 10.9, 24.3, 25.8, 26.1, 26.7, 27.4, 29.1, 62.1, 81.9, 89.1, 112.4, 131.0, 142.9, 149.8, 150.5, 182.1.

*6-Chloro-2-(hex-1-ynyl)-9-((3aR,3bR,4aS,5R,5aS)-hexahydro-2,2-dimethylbicyclo[3.1.0]hex-1(5) -eno[3,2-d][1,3]dioxol-5-yl)-9H-purine (**9**).* To a stirred solution of **12** (0.40 g, 0.60 mmol) and copper iodide (0.013 g, 0.06 mmol) in anhydrous DMF (5 mL) was added 1-iodohexyne (0.124 mL, 0.6 mmol) in DMF (4 mL) dropwise via syringe pump over a period of 1 h at room temperature, and the reaction mixture was stirred at 50 °C for 5 h. The reaction mixture was cooled to room temperature, quenched with saturated $NaHCO_3$ (5 mL) solution, and diluted with EtOAc (10 mL). The organic layer was separated, and the aqueous layer was further extracted with EtOAc (3 × 5 mL). The combined organic layers were washed with brine (5 mL) and water (5 mL), dried over anhydrous $MgSO_4$, and filtered. The solvent was evaporated under reduced pressure, and the residue was purified by flash silica gel column chromatography (hexane/EtOAc = 3: 1) to give **9** (0.155 g, 60%) as a white foam, whose spectral data were identical to those of authentic sample.

Biological Assays. *Cell Culture and Membrane Preparation.* CHO cells expressing the recombinant hA_1 or A_3R and HEK-293 cells expressing the $hA_{2A}AR$ were cultured in Dulbecco's modified Eagle's medium (DMEM) and F12 (1:1) supplemented with 10% fetal bovine serum, 100 U/ml penicillin, 100 μg/mL streptomycin, and 2 μmol/mL glutamine. RBL-2H3 cells endogenously expressing rA_3AR were cultured as described.[41] Cells were harvested by trypsinization. After homogenization and suspension, cells were centrifuged at 500*g* for 10 min, and the pellet was resuspended in 50 mM Tris·HCl buffer (pH 7.4) containing 10 mM $MgCl_2$. The suspension was homogenized with an electric homogenizer for 10 s and was then recentrifuged at 20 000*g* for 20 min at 4 °C. The resultant pellets were resuspended in buffer containing 3 U/mL adenosine deaminase, and the suspension was stored at −80 °C until the binding experiments. The protein concentration was measured using the Bradford assay.[42]

Binding Assays at the hA_1 and $hA_{2A}ARs$. For binding to the hA_1AR, 50 μL of increasing concentrations of a test ligand and 50 μL of [^{3}H]**14** (2 nM, PerkinElmer, Boston, MA) were incubated with membranes (40 μg/tube) from CHO cells stably expressing the hA_1 AR at 25 °C for 60 min in 50 mM Tris·HCl buffer (pH 7.4; $MgCl_2$, 10 mM) in a total assay volume of 200 μL.[32] Nonspecific binding was determined using 10 μM of N^6-cyclopentyladenosine (CPA, **17**). For $hA_{2A}AR$ binding, membranes (20 μg/tube) from HEK-293 cells stably expressing the $hA_{2A}AR$ were incubated at 25 °C for 60 min with a final concentration of 15 nM [^{3}H]**15** (American Radiolabeled Chemicals, Inc., St. Louis, MO) in a mixture containing 50 μL of increasing concentrations of a test ligand and 200 μL of 50 mM Tris·HCl, pH 7.4, containing 10 mM $MgCl_2$. Compound **16** (10 μM) was used to define nonspecific binding. The reaction was terminated by filtration with GF/B filters. Filters for A_1 and $A_{2A}AR$ binding were placed in scintillation vials containing 5 mL of Hydrofluor scintillation buffer and counted using a PerkinElmer Tricarb 2810TR Liquid Scintillation Analyzer.

Binding Assay at the hA_3AR and rA_3AR. Each tube in the competitive binding assay contained 100 μL membrane suspension (20 μg protein), 50 μL [^{125}I]**13** (1.0 nM, PerkinElmer, Boston, MA), and 50 μL of increasing concentrations of the test ligands in Tris·HCl buffer (50 mM, pH 8.0) containing 10 mM $MgCl_2$, 1 mM EDTA.[32] Nonspecific binding was determined using 10 μM of **16** in the buffer. The mixtures were incubated at 25 °C for 60 min. Binding reactions were terminated by filtration through Whatman GF/B filters under reduced pressure using a MT-24 cell harvester (Brandell, Gaithersburgh, MD, USA). Filters were washed three times with 9 mL ice-cold buffer. Filters for A_3AR binding were counted using a PerkinElmer Cobra II γ-counter.

Cyclic AMP Accumulation Assay. Intracellular cAMP levels were measured with a competitive protein binding method.[34] CHO cells that expressed the recombinant $hA_{2B}AR$ or hA_3AR were harvested by trypsinization. After centrifugation and resuspension in medium, cells were plated in 24-well plates in 0.5 mL medium. After 24 h, the medium was removed, and cells were washed three times with 1 mL DMEM, containing 50 mM *N*-(2-hydroxyethyl)piperazine-*N*′-2-ethanesulfonic acid (HEPES), pH 7.4. Cells were then treated with agonists and/or test compounds in the presence of rolipram (10 μM) and adenosine deaminase (3 units/mL). For assay of the hA_3AR but not the $hA_{2B}AR$, forskolin (10 μM) was added to the medium after 45 min. After the addition of forskolin, the incubation was continued an additional 15 min. The reaction was terminated upon removal of the supernatant, and cells were lysed upon the addition of 200 μL of 0.1 M ice-cold HCl. The cell lysate was resuspended and stored at −20 °C. For determination of cAMP production, protein kinase A (PKA) was incubated with [^{3}H]cAMP (2 nM) in K_2HPO_4/EDTA buffer (K_2HPO_4, 150 mM; EDTA, 10 mM), 20 μL of the cell lysate, and 30 μL 0.1 M HCl or 50 μL of cAMP solution (0−16 pmol/200 μL for standard curve). Bound radioactivity was separated by rapid filtration through Whatman GF/C filters and washed once with cold buffer. Bound radioactivity was measured by liquid scintillation spectrometry.

Statistical Analysis. Binding and functional parameters were calculated using Prism 5.0 software (GraphPAD, San Diego, CA, USA). IC_{50} values obtained from competition curves were converted to K_i values using the Cheng−Prusoff equation.[43] Data were expressed as mean ± standard error of the mean.

Antifibrosis Assay. Immortalized murine proximal tubular cells (mProx24) derived from microdissected proximal tubular segments of C57BL6/J adult mouse kidneys were supplied from Dr. Sugaya at St. Marianna University School of Medicine, Kanagawa, Japan. mProx24 were maintained in DMEM supplemented with 10% fetal calf serum (FCS; Gibco), 100 U/ml penicillin, 100 μg/mL streptomycin, and 44 mM $NaHCO_3$ under 5% CO_2 environment at 37 °C. Cells were cultured in 6-well plate for mRNA analysis. At next day after seeding cell on 6-well plate, the cultured cells were growth-arrested with a DMEM medium containing 0.15% FCS for 24h. Each synthesized compound was dissolved in DMSO to 50 mM and it was diluted to 20 mM, 10 mM, and 1 mM. After cells were pretreated with the synthesized compound dissolved in DMEM containing 0.15% FCS for 1 h, treated with recombinant human transforming growth factor-β1 (hTGF β1, R&D Systems) 5 ng/mL for 6 h. Total RNA was extracted from mProx24 using Trizol (Invitrogen) according to the standard protocol. mRNA expressions were measured by real-time PCR using StepOnePlus (Applied Biosystems) with 20 μL reaction volume consisting of cDNA transcripts, primer pairs, and SYBR Green PCR Master Mix (Applied Biosystems). Quantifications were normalized to 18S. The sequences of mouse collagen Iα1 primer pairs are 5′-GAACATCACCTACCA CTGCA-3′ and 5′-GTTGGGATGGAGG-GAGTTTA-3′.

Molecular Modeling. The X-ray crystal structure of the human A_{2A} AR in complex with an agonist, **16** (PDB ID: 2YDV)[34] was retrieved from the protein data bank (PDB) and prepared using the Protein Preparation Wizard in Maestro v9.2 (Schrödinger, LLC, NY, U.S.A.), where water and ions were removed, hydrogen atoms were added and optimized, and then the protein was minimized using the Optimized Potentials for Liquid Simulations-all atom (OPLS-AA) 2005 force field. The structures of the molecules were sketched in the Maestro and energy minimized using Impact v5.7 (Schrödinger, LLC, NY, U.S.A.) considering conjugant gradient algorithm with the maximum minimization cycles of 1000 and convergence gradient of 0.001 kJ/mol-Å. The four docking programs Glide-SP (standard precision), Glide-XP (extra precision), GOLD, and Surflex-dock showed

dx.doi.org/10.1021/jm4015313 | *J. Med. Chem.* 2014, 57, 1344−1354

consistent results, and the Glide-XP docking results are presented. The receptor grid box with 10 Å around the centroid of the cocrystallized NECA was generated. The best binding poses of **2**, **4a**, and **4f** were selected for the calculation of the receptor−ligand binding free energy (ΔG_{bind}) using Prime molecular mechanics-generalized Born surface area (MM-GBSA) module (Schrödinger, LLC, NY, U.S.A.).

The Ballesteros−Weinstein double-numbering system[44] is used to describe the transmembrane (TM) location of the amino acids. Along with numbering their positions in the primary amino acid sequence, the residues have numbers in parentheses (X.YZ) that indicate their position in each transmembrane (TM) helix (X), relative to a conserved reference residue in that TM helix (YZ).

■ ASSOCIATED CONTENT

Supporting Information

Elemental analyses, molecular docking studies in the hA_3AR homology model, and ^1H and ^{13}C NMR copies of **8**−**12** and **4a**−**4i**. This material is available free of charge via the Internet at http://pubs.acs.org.

■ AUTHOR INFORMATION

Corresponding Author

*E-mail: lakjeong@snu.ac.kr. Fax: 82-2-888-9122. Tel.: 82-2-880-7850.

Notes

The authors declare no competing financial interest.

■ ACKNOWLEDGMENTS

This research was supported by grants from Midcareer Research Program (2010-0026203 and 370C-20130120) and the National Leading Research Lab (NLRL) Program (2011-0028885) through the Ministry of Science, ICT & Future Planning (MSIP) and the National Research Foundation, Korea and in part by the Intramural Research Program of the NIH, National Institute of Diabetes and Digestive and Kidney Diseases. In this study, Schrödinger software was used and the supercomputing resources including technical support were provided by the Supercomputing Center/Korea Institute of Science and Technology Information (KSC-2011-C2-45).

■ ABBREVIATIONS:

AR, adenosine receptor; TGF, transforming growth factor; mProx, murine proximal; cAMP, cyclic adenosine-5′-monophosphate; IP_3, inositol triphosphate; DAG, diacylglycerol; AC, adenylate cyclase; PLC, phospholipase C; CKD, renin−angiotensin−aldosterone system; RAAS, Chronic kidney disease; Cl-IB-MECA, 2-chloro-N^6-(3-iodobenzyl)-5′-*N*-methylcarbamoyladenosine; thio-Cl-IB-MECA, 2-chloro-N^6-(3-iodobenzyl)-5′-*N*-methylcarbamoyl-4′-thioadenosine; LiTMP, lithium tetramethylpiperidide; CHO, Chinese hamster ovary; HEK, human embryonic kidney; I-AB-MECA, N^6-(3-iodo-4-aminobenzyl)-5′-*N*-methylcarboxamidoadenosine; R-PIA, (-)-N^6-2-phenylisopropyl adenosine; CGS21680, 2-[*p*-(2-carboxyethyl)-phenylethylamino]-5′-*N*-ethylcarboxamidoadenosine; NECA, 5′-*N*-ethylcarboxamidoadenosine; DMEM, Dulbecco's modified Eagle's medium; HEPES, *N*-(2-hydroxyethyl)piperazine-*N*′-2-ethanesulfonic acid; OPLS-AA, optimized potentials for liquid simulations-all atom; MM-GBSA, molecular mechanics-generalized born surface area; TM, transmembrane

■ REFERENCES

(1) Olah, M. E.; Stiles, G. L. The role of receptor structure in determining adenosine receptor activity. *Pharmacol. Ther.* **2000**, *85*, 55−75.
(2) Fredholm, B. B.; IJzerman, A. P.; Jacobson, K. A.; Linden, J.; Müller, C. Nomenclature and classification of adenosine receptors − An update. *Pharmacol. Rev.* **2011**, *63*, 1−34.
(3) Fredholm, B. B.; Cunha, R. A.; Svenningsson, P. Pharmacology of adenosine receptors and therapeutic applications. *Curr. Top. Med. Chem.* **2002**, *3*, 413−426.
(4) Jacobson, K. A.; Gao, Z.-G. Adenosine receptors as therapeutic targets. *Nat. Rev. Drug Discovery* **2006**, *5*, 247−264.
(5) Hasko, G.; Linden, J.; Cronstein, B.; Pacher, P. Adenosine receptors: Therapeutic aspects for inflammatory and immune diseases. *Nat. Rev. Drug Discovery* **2008**, *7*, 759−770.
(6) Schieppati, A.; Remuzzi, G. Chronic renal diseases as a public health problem: Epidemiology, social, and economic implications. *Kidney Int.* **2005**, *Suppl (98)*, S7−S10.
(7) Brenner, B. M; Cooper, M. E.; de Zeeuw, D.; Keane, W. F.; Mitch, W. E.; Parving, H. H.; Remuzzi, G.; Snapinn, S. M.; Zhang, Z.; Shahinfar, S. Effects of losartan on renal and cardiovascular outcomes in patients with type 2 diabetes and nephropathy. *N. Engl. J. Med.* **2001**, *345*, 861−869.
(8) Lewis, E. J.; Hunsicker, L. G.; Bain, R. P.; Rohde, R. D. The effect of angiotensin-converting-enzyme inhibition on diabetic nephropathy. *N. Engl. J. Med.* **1993**, *329*, 1456−1462.
(9) Vilayur, E.; Harris, D. C. H. Emerging therapies for chronic kidney disease: What is their role? *Nat. Rev. Nephrol.* **2009**, *5*, 375−383.
(10) Lee, H. T.; Ota-Setlik, A.; Xu, H.; D'Agati, V. D.; Jacobson, M. A.; Emala, C. W. A_3 adenosine receptor knockout mice are protected against ischemia-and myoglobinuria-induced renal failure. *Am. J. Physiol.: Renal, Fluid Electrolyte Physiol.* **2003**, *284*, F267−F273.
(11) Lee, J.; Hwang, I.; Ha, H. Adenosine receptors are up-regulated in unilateral ureteral obstructed rat kidneys. *Transplant. Proc.* **2012**, *44*, 1166−1168.
(12) Baraldi, P. G.; Cacciari, B.; Romagnoli, R.; Merighi, S.; Varani, K.; Borea, P. A.; Spalluto, G. A_3 adenosine receptor ligands: history and perspectives. *Med. Res. Rev.* **2000**, *20*, 103−128.
(13) Baraldi, P. G.; Preti, D.; Borea, P. A.; Varani, K. Medicinal chemistry of A_3 adenosine receptor modulators: Pharmacological activities and therapeutic implications. *J. Med. Chem.* **2012**, *55*, 5676−5703.
(14) Gallo-Rodriguez, C.; Ji, X.-D.; Melman, N.; Siegman, B. D.; Sanders, L. H.; Orlina, J.; Fischer, B.; Pu, Q.; Olah, M. E.; van Galen, P. J. M.; Stiles, G. L.; Jacobson, K. A. Structure-activity relationships of N^6-benzyladenosine-5′-uronamides as A_3-selective adenosine agonists. *J. Med. Chem.* **1994**, *37*, 636−646.
(15) Kim, H. O.; Ji, X.-D.; Siddiqi, S. M.; Olah, M. E.; Stiles, G. L.; Jacobson, K. A. 2-Substitution of N^6-benzyladenosine-5′-uronamides enhances selectivity for A_3-adenosine receptors. *J. Med. Chem.* **1994**, *37*, 3614−3621.
(16) Choi, W. J.; Lee, H. W.; Kim, H. O.; Chinn, M.; Gao, Z.-G.; Patel, A.; Jacobson, K. A.; Moon, H. R.; Jung, Y. H.; Jeong, L. S. Design and synthesis of N^6-substituted-4′-thioadenosine-5′-methyluronamides as potent and selective human A_3 adenosine receptor agonists. *Bioorg. Med. Chem.* **2009**, *17*, 8003−8011.
(17) (a) Jeong, L. S.; Jin, D. Z.; Kim, H. O.; Shin, D. H.; Moon, H. R.; Gunaga, P.; Chun, M. W.; Kim, Y.-C.; Melman, N.; Gao, Z.-G.; Jacobson, K. A. N^6-Substituted D-4′-thioadenosine-5′-methyluronamides: potent and selective agonists at the human A_3 adenosine receptor. *J. Med. Chem.* **2003**, *46*, 3775−3777. (b) Jeong, L. S.; Lee, H. W.; Jacobson, K. A.; Kim, H. O.; Shin, D. H.; Lee, J. A.; Gao, Z.-G.; Lu, C.; Duong, H. T.; Gunaga, P.; Lee, S. K.; Jin, D. Z.; Chun, M. W.; Moon, H. R. Structure−activity relationships of 2-chloro-N^6-substituted-4′-thioadenosine-5′-methyluronamides as highly potent and selective agonists at the human A_3 adenosine receptor. *J. Med. Chem.* **2006**, *49*, 273−281.

(18) DeNinno, M. P.; Masamune, H.; Chenard, L. K.; DiRico, K. J.; Eller, C.; Etienne, J. B.; Tickner, J. E.; Kennedy, S. P.; Knight, D. R.; Kong, J.; Oleynek, J. J.; Tracey, W. R.; Hill, R. J. 3′-Aminoadenosine-5′-uronamides: Discovery of the first highly selective agonist at the human adenosine A_3 receptor. *J. Med. Chem.* **2003**, *46*, 353−355.
(19) Volpini, R.; Costanzi, S.; Lambertucci, C.; Taffi, S.; Vittori, S.; Klotz, K. N.; Cristalli, G. N^6-alkyl-2-alkynyl derivatives of adenosine as potent and selective agonists at the human adenosine A_3 receptor and a starting point for searching A_{2B} ligands. *J. Med. Chem.* **2002**, *45*, 3271−3279.
(20) (a) Melman, A.; Wang, B.; Joshi, B. V.; Gao, Z.-G.; de Castro, S.; Heller, C. L.; Kim, S.-K.; Jeong, L. S.; Jacobson, K. A. Selective A_3 adenosine receptor antagonists derived from nucleosides containing a bicyclo[3.1.0]hexane ring system. *Bioorg. Med. Chem.* **2008**, *16*, 8546−8556. (b) Jeong, L. S.; Choe, S. A.; Gunaga, P.; Kim, H. O.; Lee, H. W.; Lee, S. K.; Tosh, D. K.; Patel, A.; Palaniappan, K. K.; Gao, Z.-G.; Jacobson, K. A.; Moon, H. R. Discovery of a new nucleoside template for human A_3 adenosine receptor ligands: D-4′-thioadenosine derivatives without 4′-hydroxymethyl group as highly potent and selective antagonists. *J. Med. Chem.* **2007**, *50*, 3159−3162. (c) Jeong, L. S.; Pal, S.; Choe, S. A.; Choi, W. J.; Jacobson, K. A.; Gao, Z.-G.; Klutz, A. M.; Hou, X.; Kim, H. O.; Lee, H. W.; Tosh, D. K.; Moon, H. R. Structure−activity relationships of truncated D- and L-4′-thioadenosine derivatives as species-independent A_3 adenosine receptor antagonists. *J. Med. Chem.* **2008**, *51*, 6609−6613. (d) Pal, S.; Choi, W. J.; Choe, S. A.; Heller, C. L.; Gao, Z.-G.; Chinn, M.; Jacobson, K. A.; Hou, X.; Lee, S. K.; Kim, H. O.; Jeong, L. S. Structure−activity relationships of truncated adenosine derivatives as highly potent and selective human A_3 adenosine receptor antagonists. *Bioorg. Med. Chem.* **2009**, *17*, 3733−3738.
(21) Wang, Z.; Do, C. W.; Avila, M. Y.; Peterson-Yantorno, K.; Stone, R. A.; Gao, Z.-G.; Joshi, B.; Besada, P.; Jeong, L. S.; Jacobson, K. A.; Civan, M. M. Nucleoside-derived antagonists to A_3 adenosine receptors lower mouse intraocular pressure and act across species. *Exp. Eye Res.* **2010**, *90*, 146−154.
(22) (a) Hou, X.; Kim, H. O.; Alexander, V.; Kim, K.; Choi, S.; Park, S.; Lee, J. H.; Yoo, L. S.; Gao, Z.; Jacobson, K. A.; Jeong, L. S. Discovery of a new human A_{2A} adenosine receptor agonist, truncated 2-hexynyl-4′-thioadenosine. *ACS Med. Chem. Lett.* **2010**, *1*, 516−520. (b) Hou, X.; Majik, M. S.; Kim, K.; Pyee, Y.; Lee, Y.; Alexander, V.; Chung, H.-W.; Lee, H. W.; Chandra, G.; Lee, J. H.; Park, S.-g; Choi, W. J.; Kim, H. O.; Phan, K.; Gao, Z.-G.; Jacobson, K. A.; Choi, S.; Lee, S. K.; Jeong, L. S. Structure−activity relationships of truncated C2- or C8-substituted adenosine derivatives as dual acting A_{2A} and A_3 adenosine receptor ligands. *J. Med. Chem.* **2012**, *55*, 342−356.
(23) Kang, S.-K.; Kim, W.-Y.; Jiao, X. Copper-catalyzed cross-coupling of 1-iodoalkynes with organostannanes. *Synthesis* **1998**, 1251−1254.
(24) Chinchilla, R.; Nájera, C. The Sonogashira reaction: A booming methodology in synthetic organic chemistry. *Chem. Rev.* **2007**, *107*, 874−922.
(25) Xu, Q.; Norman, J. T.; Shrivastav, S.; Lucio-Cazana, J.; Kopp, J. B. In vitro models of TGF-beta-induced fibrosis suitable for high-throughput screening of antifibrotic agents. *Am. J. Physiol.: Renal, Fluid Electrolyte Physiol.* **2007**, *293*, F631−F640.
(26) (a) Choi, W. J.; Park, J. G.; Yoo, S. J.; Kim, H. O.; Moon, H. R.; Chun, M. W.; Jung, Y. H.; Jeong, L. S. Syntheses of D- and L-cyclopentenone derivatives using ring-closing metathesis: Versatile intermediates for the synthesis of D- and L-carbocyclic nucleosides. *J. Org. Chem.* **2001**, *66*, 6490−6494. (b) Moon, H. R.; Choi, W. J.; Kim, H. O.; Jeong, L. S. Improved and alternative synthesis of D- and L-cyclopentenone derivatives, the versatile intermediates for the synthesis of the carbocyclic nucleosides. *Tetrahedron: Asymmetry* **2002**, *13*, 1189−1193.
(27) Choi, M. J.; Chandra, G.; Lee, H. W.; Hou, X.; Choi, W. J.; Phan, K.; Jacobson, K. A.; Jeong, L. S. Regio- and stereoselective synthesis of truncated 3′-aminocarbanucleosides and their binding affinity at the A_3 adenosine receptor. *Org. Biomol. Chem.* **2011**, *9*, 6955−6962.
(28) (a) Kato, K.; Hayakawa, H.; Tanaka, H.; Kumamoto, H.; Shindoh, S.; Shuto, S.; Miyasaka, T. A new entry to 2-substituted purine nucleosides based on lithiation-mediated stannyl transfer of 6-chloropurine nucleosides. *J. Org. Chem.* **1997**, *62*, 6833−6841. (b) Brun, V.; Legraverend, M.; Grierson, D. S. Cyclin-dependent kinase (CDK) inhibitors: development of a general strategy for the construction of 2,6,9-trisubstituted purine libraries. Part 1. *Tetrahedron Lett.* **2001**, *42*, 8161−8164. (c) Taddei, D.; Kilian, P.; Slawin, A. M. Z.; Woollins, D. Synthesis and full characterization of 6-chloro-2-iodopurine, a template for the functionalisation of purines. *Org. Biomol. Chem.* **2004**, *2*, 665−670.
(29) Tosh, D. K.; Chinn, M.; Ivanov, A. A.; Klutz, A. M.; Gao, Z. G.; Jacobson, K. A. Functionalized congeners of A_3 adenosine receptor-selective nucleosides containing a bicyclo[3.1.0]hexane ring system. *J. Med. Chem.* **2009**, *52*, 7580−7592.
(30) (a) Moon, H. R.; Kim, H. O.; Chun, M. W.; Jeong, L. S.; Marquez, V. E. *J. Org. Chem.* **1999**, *64*, 4733−4741. (b) Marquez, V. E. In *Modified Nucleosides: in Biochemistry, Biotechnology and Medicine*; Herdewijn, P., Ed.; Wiley-VCH Verlag GmbH & Co. KGaA: Weinheim, 2008, pp 307−341.
(31) Sonogashira, K. Development of Pd-Cu catalyzed cross-coupling of terminal acetylenes with sp2-carbon halides. *J. Organomet. Chem.* **2002**, *653*, 46−49.
(32) (a) Perreira, M.; Jiang, J. K.; Klutz, A. M.; Gao, Z. G.; Shainberg, A.; Lu, C.; Thomas, C. J.; Jacobson, K. A. Reversine and its 2-substituted adenine derivatives as potent and selective A_3 adenosine receptor antagonists. *J. Med. Chem.* **2005**, *48*, 4910−4918. (b) Jarvis, M. F.; Schutz, R.; Hutchison, A. J.; Do, E.; Sills, M. A.; Williams, M. [^{3}H]CGS 21680 a selective A_2 adenosine receptor agonist directly labels A_2 receptors in rat brain. *J. Pharmacol. Exp. Ther.* **1989**, *251*, 888−893. (c) Olah, M. E.; Gallo-Rodriguez, C.; Jacobson, K. A.; Stiles, G. L. ^{125}I-4-Aminobenzyl-5′-N-methylcarboxamidoadenosine a high affinity radioligand for the rat A_3 adenosine receptor. *Mol. Pharmacol.* **1994**, *45*, 978−982.
(33) (a) Tchilibon, S.; Joshi, B. V.; Kim, S. K.; Duong, H. T.; Gao, Z. G.; Jacobson, K. A. (*N*)-Methanocarba 2,N^6-disubstituted adenine nucleosides as highly potent and selective A_3 adenosine receptor agonists. *J. Med. Chem.* **2005**, *48*, 1745−1758. (b) Lee, K.; Ravi, R. G.; Ji, X.-D.; Marquez, V. E.; Jacobson, K. A. Ring-constrained (*N*)-methanocarba-nucleosides as adenosine receptor agonists: Independent 5′-uronamide and 2′-deoxy modifications. *Bioorg. Med. Chem. Lett.* **2001**, *11*, 1333−1337.
(34) Nordstedt, C.; Fredholm, B. B. A modification of a protein-binding method for rapid quantification of cAMP in cell-culture supernatants and body fluid. *Anal. Biochem.* **1990**, *189*, 231−234.
(35) Lebon, G.; Warne, T.; Edwards, P. C.; Bennett, K.; Langmead, C. J.; Leslie, A. G.; Tate, C. G. Agonist-bound adenosine A_{2A} receptor structures reveal common features of GPCR activation. *Nature* **2011**, *474*, 521−525.
(36) Kim, S. K.; Gao, Z. G.; Van Rompaey, P.; Gross, A. S.; Chen, A.; Van Calenbergh, S.; Jacobson, K. A. Modeling the adenosine receptors: Comparison of the binding domains of A_{2A} agonists and antagonists. *J. Med. Chem.* **2003**, *46*, 4847−4859.
(37) Kim, J.; Wess, J.; van Rhee, A. M.; Schöneberg, T.; Jacobson, K. A. Site-directed mutagenesis identifies residues involved in ligand recognition in the human A_{2A} adenosine receptor. *J. Biol. Chem.* **1995**, *270*, 13987−13997.
(38) Dal Ben, D.; Lambertucci, C.; Marucci, G.; Volpini, R.; Cristalli, G. Adenosine receptor modeling: what does the A_{2A} crystal structure tell us? *Curr. Top. Med. Chem.* **2010**, *10*, 993−1018.
(39) Fujioka, M.; Omori, N. Subtleties in GPCR drug discovery: a medicinal chemistry perspective. *Drug Discovery Today* **2012**, *17*, 1133−1138.
(40) Lee, J.; Hwang, I.; Lee, J. H.; Lee, H. W.; Jeong, L. S.; Ha, H. J. The selective A_3AR antagonist LJ-1888 ameliorates UUO-induced tubulointerstitial fibrosis. *Am. J. Pathol.* **2013**, *183*, 1488−1497.
(41) Park, K. S.; Hoffmann, C.; Kim, H. O.; Padgett, W. L.; Daly, J. W.; Brambilla, R.; Motta, C.; Abbracchio, M. P.; Jacobson, K. A. Activation and desensitization of rat A_3-adenosine receptors by

selective adenosine derivatives and xanthine-7-ribosides. *Drug Dev. Res.* **1998**, *44*, 97−105.
(42) Bradford, M. M. A rapid and sensitive method for the quantitation of microgram quantities of protein utilizing the principle of protein-dye binding. *Anal. Biochem.* **1976**, *72*, 248−254.
(43) Cheng, Y.-C.; Prusoff, W. H. Relationship between the inhibition constant (K_i) and the concentration of inhibitor which causes 50% inhibition (IC_{50}) of an enzymatic reaction. *Biochem. Pharmacol.* **1973**, *22*, 3099−3108.
(44) Ballesteros, J. A.; Weinstein, H.; Stuart, C. S. In *Receptor Molecular Biology*; Sealfon, S. C., Ed.; Academic Press: San Diego, CA, 1995; pp 366−428.